Heavy Naphtha Reforming Reactions with Tri-metallic Catalysts, Experimental and Analytical Investigation

Dr. Shahrazad R.Raouf *, Dr.Khalid A.Sukkar**
& Dr. Ramzy S.Hamied**

Received on: 18/10/2010
Accepted on: 2/6/2011

Abstract

In present work experimental and theoretical studies (A comprehensive mathematical model and simulation was developed to describe the reaction kinetics in catalytic reforming process) have been carried out on tri-metal supported on Al_2O_3 catalysts using catalytic reforming process. The Iraqi heavy naphtha is used as a feedstock for the process. The dehydrogenation, dehydrocyclization, and hydrocracking reaction were investigated to characterize the catalysts performance toward higher activity and selectivity to desired products. The performance of catalysts was studied under the following operating condition: weight hour space velocity in the range of (1-2 hr^{-1}), reaction temperature in the range of (480-510 °C). The results showed that the conversion of heavy naphtha components (Paraffin's and Naphthenes) increases with increasing of reaction temperature and decreases with increasing of weight hour space velocity. Also, it was noted that the yield of aromatics and light component increases for the two types of catalysts at the same condition. The concentration, conversion, and temperature profiles have been studied of and the results show a good agreement between experimental and simulation model with a deviation ranging between 4. 18% to 19.50%.

تفاعلات التهذيب لمادة النفثا الثقيلة باستخدام عوامل مساعدة ثلاثية المعدن, دراسة تجريبية وتحليلية

الخلاصة

تـضمن البحـث اعـداد دراســة شـاملة عمليــة ونظريــة للعوامـل المسـاعدة ثلاثيـة المعـدن المحملة على الالومينا المستخدمة في عملية التهذيب باستخدام مـادة النفثـا الثقيـلة (العراقيـة) كمـادة اوليـة للعمليـة .مـن اجـل دراسـة امكانيـة زيـادة كفـاءة العمليـة وتحسـين أنتقائيـة العوامـل المساعدة تم خلال البحث دراســة التفاعـلات الرئيسية التي تحدث في عملية التهذيب وهي (تفاعــلات ازالــة الهيـدروجين, تفـاعلات تكـوين المركبـات الحلقيـة وكـذلك تفاعــلات التكسـير الحـراري) بوجـود الهيـدروجين. تـم دراسـة اداء نـوعين مـن العوامـل المسـاعدة الثلاثيـة المعـدن حسب الضروف التشغيلية التالية : السرعة الفراغية للغاز(2-1 ساعة$^{-1}$) , درجة حرارة التفاعل تتراوح بين (510-480 م°). أثبتت النتـائج العمليـة ان نسـبة التحـول لمـادة النفثـا الثقيلـة (المـواد البرافينيـة والمـواد النفثينيـة) تـزداد مـع زيـادة درجـة حـرارة التفاعـل وتقـل مـع زيـادة السـرعة الفراغيـة. كـذلك لـوحظ ان الانتاجيـة (yield) للمـواد العطريـة والمركبـات الخفيفـة تـزداد لجميـع انواع العوامل المساعدة المحضرة. أثبتت النتـائج وجـود تطـابق كبيـر بـين النتـائج العمليـة للبحـث

* Chemical Engineering Department, University of Technology/ Baghdad.
** Petroleum Technology Department, University of Technology/ Baghdad

والنتائج النظرية ونسبة أنحراف تتراوح بين (% 4.18 - % 19.50) وذلك من خلال دراسة (توزيع التراكيزللمواد الداخلة والناتجة, نسبة التحول, وتوزيع درجة الحرارة).

1. Introduction

Catalytic naphtha reforming unit is the heart of many modern refineries. They are the main procedures of high octane naphtha (approximately 40% of the world production comes from catalytic reforming units) and aromatic hydrocarbons and they are a very important source of hydrogen [1, 2].

The purpose of catalytic reforming of naphtha is primarily to increase the octane number of the naphtha feedstock to the level that makes the reformate product suitable as a gasoline blend stock [3, 4].

During catalytic reforming long chain hydrocarbons are rearranged through dehydrocyclization dehydrogenation isomerization, hydrocracking, and reactions. These reactions occur on acid and/or metal sites and they demand the use of bifunctional catalysts. The acid function is typically provided by a solid support such as chlorinated alumina (Al_2O_3–Cl) and the metal function by a noble metal. The metal component is active for the Hydrogenation and dehydrogenation reactions while the support has the acid strength necessary to promote the isomerization reactions. Synergetic action of both kinds of active sites promotes other reactions such as dehydrocyclization via a bifunctional reaction mechanism. Undesirable reactions such as hydrocracking and hydrogenolysis also occur lowering the yield of valuable products and deactivating the catalyst by the formation of coke on the active sites [5, 6, and 7].

Many different types of reforming catalysts were developed such as bi-metals and tri-metals supported catalysts. The advantage of the use of trimetallic catalysts over classic Pt-Re bimetallic catalysts is their lower coking rate and their higher resistance to deactivation. These factors enable the process to be operated with smaller regeneration frequencies leading to a subsequent reduction of operating costs. [2].

Therefore, in catalytic reforming it is very important to develop an appropriate kinetic model capable of predicting the detailed reformat composition and behaviors of catalysts in order to combine with catalytic reforming reactor model, for simulation and optimization purposes [8]. It is important to mention here that, many authors studied the design and simulation of catalytic reforming in Iraq like (Jamali J.S., Mohammed A.A., and Raouf S.R.) [9, 10, and 11]. The aim of this work is to produce high octane aromatics with adding hydrogen from Iraqi heavy naphtha by using prepared tri-metallic catalysts in a fixed bed reactor with various ranges of temperatures and weight hour space velocity. A mathematical model has been Adeveloping to describe the catalytic reforming reactions,

reaction rate and optimum operating conditions for the reforming catalysts.

2. Mathematical Model and Theoretical Aspects

2.1 Model Description and Assumption

The main aim of the present study was to analyze the kinetics of reforming which involved heavy naphtha raw material. Therefore three groups of compounds are found which are: Paraffin's (normal and iso), naphthenes (N), and Aromatics (A). Thus, it was possible to predict the content of the defined reagents in the course of the process for an arbitrary temperature within the investigated range. The physical model for catalytic reforming with mass and energy balance for the element combining kinetic thermodynamic, concentration, and temperature distributions along the reactor length can be calculated. In developing the model of the catalytic reforming reactor the following assumptions are taken into account.

- Steady state operation, one dimensional and plug flow isothermal operation.
- The pressure is constant throughout the reactor.
- Limiting reactant in gas phase.
- The temperature and concentration gradients along the radial direction can be neglected and only axial direction variables are considered.
- All the reforming reactions rates are first order (proved experimentally), all the rate equations are linear pseudo-monomolecular in nature and constant catalyst activity for calculation.

2.2 Reaction Kinetics

Heterogeneous reaction (consecutive and parallel) of heavy naphtha is used to model catalytic reforming performance as shown in Figure (1) and written as follows:-

$\mathbf{P \leftrightarrow N + H_2}$ **….(1)**

$\mathbf{N \rightarrow A + 3H_2}$ **….. (2)**

$\mathbf{P + H_2 \rightarrow 2G}$ **……(3)**

The kinetic reaction rate is considered to follow simple power law kinetic expression for above reactions [12]:

$$r_1 = k_1 C_P - k_3 C_N P_{H_2} \quad \textbf{….(4)}$$

$$r_2 = k_2 C_N \quad \textbf{….. (5)}$$

$$r_3 = k_4 C_P \quad \textbf{….. (6)}$$

In general form

$$r_i = k_i C_i \quad \textbf{…….(7)}$$

Where

$$k_i = A_\circ EXP\left(\frac{-E_a}{R.T}\right) \text{[12]} \quad \textbf{….(8)}$$

The reaction rate constant k_i confirms the Arrhenius expression:-

$$Lnk_i = LnA_\circ - \frac{E_a}{R.T} \quad \textbf{….. (9)}$$

The reaction equilibrium constants $K_{eq} = k_1/k_3$.

Therefore, equilibrium constant can be calculated by the following thermodynamic relation:

$$K_{eq} = EXP\left(\frac{-\Delta G}{R.T}\right) \text{[13]} \quad \textbf{….(10)}$$

The kinetic expression is to be linear (first order with respect to reactants) under the present reactions.

2.3 Kinetic Reaction Model

The feed to the catalytic reforming process is generally heavy naphtha cut and in this model, the naphtha feed is characterized into PNA (Paraffin's, Naphthenes, and Aromatics), this reactions net work is shown in Figure (1), and to best describe the reaction, here the Langmuir-Hinshelwood adsorption model is employed as shown in figure (1) to describe the reaction.

2.3.1 Mass Balance

To develop the reaction model for an integral reactor, a material balance is made over a small element, of the tubular catalyst bed, Figure (2); the resulting equation is:-

$$\mathbf{F_N}\Big|_{z} \; \mathbf{-\; F_N}\Big|_{z+\Delta z} \; \mathbf{-\; V_P\,(-r_i) = 0} \quad [14]$$

……(11)

As $\Delta z \rightarrow 0$, the differential material balance reduces to:-

$$\frac{dF_n}{dV} = -r_i \qquad \text{…..(12)}$$

The reaction rate equations are developed for each component in heavy naphtha feed stocks (Paraffin's, Naphthenes and Aromatics) and defining a space time variable, θ, as:-

$$\theta = V_C/f \qquad \text{…… (13)}$$

For a constant feed rate, an incremental section of catalyst bed, may expressed as:-

$$dV = f.d\theta \qquad \text{….. (14)}$$

Substituting equation (14) into equation 12:-

$$\frac{dF_P}{d\theta} = k_3 F_N - (k_4 + k_1) F_P \quad \textbf{.(15)}$$

$$\frac{dF_N}{d\theta} = k_1 F_P - (k_3 + k_2) F_N \quad \textbf{.(16)}$$

$$\frac{dF_A}{d\theta} = k_2 F_N \qquad \textbf{….(17)}$$

2.3.2 Energy Balance

The equation used to estimate the temperature profile along the reactor is obtained from an energy balance over the differential reactor control volume [15].

$$f.\rho.Cp.dT = r_{P\leftrightarrow N}.\Delta H_{r,P\leftrightarrow N}.dV + r_{N\leftrightarrow A}.\Delta H_{r,N\leftrightarrow A}.dV + r_{P\rightarrow G}.\Delta H_{r,P\rightarrow G}.dv \qquad \text{……(18)}$$

Substitution equations (17) in to equation 21 then:-

$$\frac{dT}{d\theta} = \frac{1}{\rho C_P}\left(r_{P\leftrightarrow N}\Delta H_{r,P\leftrightarrow N} + r_{N\rightarrow A}\Delta H_{r,N\rightarrow A} + r_{P\rightarrow G}\Delta H_{P\rightarrow G}\right) \quad \textbf{(19)}$$

The above differential equation is taken as first order and this is improved experimentally as:-

$$-r_i = k_i C_i$$

Taking Ln for both side of above equation yield:

$$Ln(-r_i) = Lnk_i + LnC_i \quad \textbf{…..(20)}$$

Plotting Ln ($-r_i$) vs. LnC_i, shows a straight line behavior, Figure (3) and (4) different reactions and different catalyst. These two figures samples for two catalysts.

2.4 Process Model (Model of Reactor)

The physical model for catalytic reforming axial flow reactor is shown in Figure (2). The ordinary differential equations for mass and

energy balance were integrated through each reactor bed to describe reformate composition and temperature profile along the length of the reactor. The system is numerically solved by method of finite difference approach with explicit solution of all the differential equation in the mathematical model (Matlab 7 version environmental).

For Mass balance:

$$\frac{dY_i}{dZ} = \sum_{i=1}^{m} \frac{MW}{z.WHSV}(-r_i) \text{ [16]. } \textbf{(21)}$$

If substitute's heavy naphtha components (Paraffin, Naphthene, and Aromatic) then equation (24) becomes:

$$\frac{dY_P}{dZ} = \frac{MW}{z.WHSV}[r_{N\to P} - (r_{P\to N} + r_{P\to G})] \textbf{(22)}$$

$$\frac{dY_N}{dZ} = \frac{MW}{z.WHSV}[r_{P\to N} - (r_{N\to P} + r_{N\to A})] \textbf{.(23)}$$

$$\frac{dY_A}{dZ} = \frac{MW}{z.WHSV}(r_{N\to A}) \textbf{ …(24)}$$

For energy balance:

$$\frac{dT}{dZ} = S\frac{\sum_{I=1}^{m} r_i(-\Delta H_{r_i})}{\sum_{I=1}^{m} f_i C_{P_i}} \text{ [16] } \textbf{…..(25)}$$

$$\frac{dT}{dZ} = \frac{S}{\sum_{I=1}^{m} f_i C_{P_i}} \begin{bmatrix} r_{P\to N}(-\Delta H_{r,P\to N}) + \\ r_{N\to A}(-\Delta H_{r,N\to A}) + \\ r_{N\to P}(-\Delta H_{r,N\to P}) \\ + r_{P\to G}(-\Delta H_{P\to G}) \end{bmatrix} \textbf{(26)}$$

$$\Delta H^{\circ}_{r,T} = \Delta H^{\circ}_{r,298} + \int_{298}^{T} \Delta C_p dT \text{ [17] ..(27)}$$

The results of heat reactions estimation shown in table (1).

3. Experimental Work

3.1 Materials

3.1.1 Naphtha feedstock

Iraqi heavy naphtha with 0.733 specific gravity was obtained from Al-Dura refinery. The properties of this naphtha are tabulated in Table (2).

3.1.2 Catalysts and Support

Pt/ γ-Al_2O_3 (RG 412), Pt-Re/ γ-Al_2O_3 (RG 482) catalysts are obtained from Al-Dura refinery. The bi-metals and tri-metal catalysts were prepared in our laboratory. The physical and chemical property of these two catalysts is given in Table (3).

3.2 Preparation of Tri-Metal Catalyst

3.2.1 Preparation of Platinum-Rhenium-Tin / Alumina Catalyst

The Pt-Re-Sn/ Al_2O_3 catalyst was prepared by co-impregnation by adding tin chloride ($SnCl_2.2H_2O$) to platinum- rhenium supported on alumina catalyst in order to reach final concentration of 0.3 wt% Pt, 0.3 wt% Re and 0.1 wt% Sn [1].

$SnCl_2$ was first dissolved in deionized water and heated for 30 min at 70 °c. Tin chloride was added to the solution containing catalyst and leaving it without stirring for 1 hr and then gently stirred for (1/2-1 hr) in water bath at 70 °C. Then, the catalyst was dried at 120 °C for 12 hrs, and calcined in air at 500 °C for 4 hrs and finally reduced in hydrogen at 500 °C for 4 hrs at hydrogen flow of 80 cm^3/min.

3.2.2 Preparation of Platinum-Iridium-Tin / Alumina Catalyst

The Pt-Ir-Sn/ Al_2O_3 catalyst was prepared by using successive impregnation by adding iridium chloride ($IrCl_3$) to platinum supported on alumina catalyst and then adding tin chloride ($SnCl_2$) in order to reach final concentration of 0.35 wt% Pt, 0.1 wt% Ir, and 0.3 wt% Sn [18].

Pt-Ir supported on alumina was mixed with 0.2M HCl (37%) to assure homogeneous distribution with stirring for 1 hr at room temperature. The tin chloride solution was added to the homogenized catalyst with gently stirred for 1 hr, and then heated at 70 $^{\circ}$C in water bath without stirring. The catalyst was finally dried at 120 $^{\circ}$C for 16 hrs and calcined in air at 500 $^{\circ}$C for 4 hrs; finally the catalyst was reduced in flowing hydrogen at 500 $^{\circ}$C for 4 hrs with hydrogen flow rate of 60 cm^3/min.

3.3Catalysts Performance

All the catalysts were originally in the form of extrudate. Each type was activated inside the reactor, just prior running the test runs. the reactivation it was 450 and 500 $^{\circ}$C for 4 hr respectively in a current of hydrogen at 1 atm pressure and flow ratio of 60 and 80 cm^3/min.

3.4 Heavy Naphtha Unit

The catalytic activities studied were carried out in a conventional continuous flow vertical tubular reactor under different reforming conditions as shown in Figure (5).

3.5 Operating Procedure

Heavy naphtha pumped under pressure to the reforming unit. Hydrogen purified by passing it over molecular sieve type (5A) and it is mixed with hydrocarbon before the reactor inlet. The mixture is preheated before entering the reactor, and then passes through the catalyst bed. The products are cooled by cooling system and collected in the separator in order to separate the un- condensed gases from the top to the atmosphere and the condensed liquid from bottom of the separator. The products samples are analyzed using gas chromatograph type Shimadzu 2014 GC. The oven is temperature programmed the concentration and retention time and other information are shown in Tables (4 ,and 5)..

The catalysts bed was tested temperatures (480, 490, 500, and 510 $^{\circ}$C), and 6 atm. The WHSV were varied at (1, 1.5, and 2 hr^{-1}), and 4:1 hydrogen to hydrocarbon molar ratio. Fresh catalyst was used in each run, therefore deactivation of catalysts will not be need to study in this investigation.

4. Results and Discussions

4.1 Effect of Temperature

The influence of reaction temperatures was between (480, 490, 500, and 510 $^{\circ}$C). The WHSV of ($1hr^{-1}$) for two types of catalyst was used.

The result in Figures (6, 7, 8, and 9) show that the concentrations of light components paraffin's (n and iso) P_5 and P_6 is increased with increasing the reaction temperature. Also illustrates that, the heavier components concentration % decrease as reaction temperature

increases, this behavior is due to the dehydrocyclization reaction which is favored at high reaction temperature and high molecular weight of carbon number [16].

Figure (10, 11, 12, and 13) shows that naphthenes mole % decreases as reaction temperature increases, the reactivity of dehydrogenation reactions increases with an increase in naphthenes carbon number [16], which increase the mole percentage of aromatics components.

4.2 Effect of Weight Hour Space Velocity

The influence of WHSV studied in the range of (1, 1.5, and 2 hr^{-1}), at reaction temperature of (510 ˚C). It was observed that this reaction temperature gives the highest aromatics yield.

Figures (14, 15, 16, and 17) show that the mol % of light component paraffins (n and iso) P_5 and P_6 decreases as WHSV increases; this increase cause a decrease in the residence time [10]. Also the heavier paraffin's (n and iso) reactivity decreases as WHSV increases which lead to a decrease in the aromatics yield, dehydrocyclization reaction of Paraffins (n and iso), is the slowest reaction and is affected by the increasing of WHSV [21], as shown in figure (20, 21). Naphthenes components conversion show a slight decrease with increasing WHSV this attributed to the dehydrogenation reaction is the fastest reaction in all heavy naphtha reforming reactions [15], as shown in figure (18, 19).

5.1 Estimation of Reaction Kinetic Parameters

The apparent activation energy (E_a) is established from Arrhenius equation as given in equations (7,8,and 9):

A plot of $Ln(k)$ vs.(1/T) is shown in Figure (22) and (23) for Pt-Ir-Sn/ Al_2O_3, these two figures show that the slope is represented by ($-E_a/R.T$) and the intercept is represented by $Ln(A_\circ)$ which means that the value of pre-exponential factor. The results of the analysis of the parameters estimation for the two types of catalysts are outlined in Table (6).

5.2 Simulation Results of Mathematical Model and Discussion

Figures (24) and (25) show the concentration profiles for reactants (Paraffins and Naphthenes) and products (Aromatics and Gases) for two catalyst type at temperature of (480 ˚C) and WHSV of ($1hr^{-1}$) along the catalyst bed length as an example.

Figure (26) shows the comparison between the results of experimental work and simulation of conversion for reactant (Paraffin). Table (7) shows the comparison between theoretical and experimental results for the two types of catalysts.

The results of Figure (27) give the trend of temperature profile which decreases along the catalyst bed length (distance), for all temperature ranges. This trend agrees with the published results

for heavy naphtha catalytic reforming process [22, and 23].

Conclusions

The addition of tin (Sn) and iridium (Ir) to Pt/ γ-Al_2O_3 and Pt-Re/ γ-Al_2O_3 catalyst as tri-metal Pt-Re-Sn/ Al_2O_3, and Pt-Ir-Sn/ Al_2O_3 improves the conversion of heavy naphtha reactants (Paraffins and Naphthenes). On the other hand, the selectivity of catalysts toward aromatization reactions especially light aromatics (A_6, and A_7) is increased.

The conversion of heavy naphtha reactants (Paraffins and Naphthenes) increases with increasing of reaction temperature in the range (480 – 510 °C), for the catalyst (Pt-Ir-Sn/ Al_2O_3) the total conversion % increases from (12.89 % - 24.06 %) for (Paraffins) and 54 % to 64.77 % for (Naphthenes), while for the catalyst (Pt-Re-Sn/ Al_2O_3) the total conversion % increases from (11.50 % - 22.58 %) for (Paraffins) and (56 % - 67 %) for (Naphthenes),and it decreases with increasing of weight hour space velocity above (1 hr^{-1}). The yield of the desired products (Aromatics) increases with increasing of reaction temperature in the range (480 – 510 °C), thus for (Pt-Re-Sn/ Al_2O_3) catalyst yield increases from 25.8 % to 32.12 %, while for (Pt-Ir-Sn/ Al_2O_3) catalyst the yield increases from (26.35 % - 31.7 %) and the latter decreases with increasing of weight hour space velocity. The derived model and simulation agrees with the experimental work results according to the suggested scheme of reactions network for heavy naphtha reforming. And the comparison of model results with experimental results shows a deviation range of 4.18 % to 19.50 %.

References

[1]Pieck C.L., Carlos R.V., Parera M.,Gustavo N.G., Luciano R.S., Luciene S.C., and Maria C.R.," Metal Dispersion and Catalytic Activity of Trimetallic Pt-Re-Sn/ Al_2O_3 Naphtha Reforming Catalysts ",J.Catal. Today, vol 107-108, 30 0ct, p 637, 2005.

[2]Silvana A.D., Carlos R.V., Florence E., Catherine E., Patrice M., Carlos L.P.," Naphtha Reforming Pt-Re-Ge/ γ-Al_2O_3 Catalysts Prepared by Catalytic Reduction (Influence of the pH of the Ge Addition Step) ", J. Catal Today, vol 133-135, p 13-19, 2008.

[3]ntos G.J, Aitani A.M, Parera J.M., Figoli N., " Catalytic Naphtha Reforming ", Marcel Dekker, Inc, New York, 2nd Edition 1995.

[4]Tore L., Sigurd S.," Data Reconciliation and Optimal Operation of A Catalytic Naphtha Reformer", J. Process Control, Sept, 2007.

[5]Viviana B., Marieme B., Vanina A.M., Catherine E., Florence E., Carlos R.V., Patrice M., Carlos L.P.," Preparation of Tri-metallic Pt-Re-Ge/ Al_2O_3 and Pt-Re-Sn/ Al_2O_3 Naphtha Reforming Catalysts by Surface Redox Reaction ", J. Appl. Catal A: vol 319, p 210-217, 2007.

[6]Meyers R.A.," HandBook of Petroleum Refining Processing", McGraw Hill, 3rd Edition, Copyrighted Material, USA 2006.

[7]Seif Mohaddecy S.R., Zahedi S., Sadighi S., Bonyad H.," Reactor Modeling and Simulation of Catalytic Reforming Process ", J. Petroleum and Coal, vol 48, No3, p 28-35, 2006.

[8]Weifeng H., Hongye S., Yongyou H., and Tiom C.," Modeling, Simulation and Optimization of a whole Industrial Catalytic Naphtha Reforming Process on Aspen plus Platform", Chinese, J.Chem. Eng, vol 14, No 5, p 584, 2006.

[8]Jamali J.S., AL-Sammerrai D.," Evaluation of the Thermal Stability of some Reforming Catalysts ", Thermodynamica Acta, Elsevier SciencePublishers B.V., Amsterdam, 127, p 217-222 , 1988.

[9]Mohammed A.A., Hussein K.H.," Catalytic Aromatization of Naphtha Using Different Catalysts", Iraq. J. Chem. and Petr Eng, vol 5, (Dec), p 13, 2004.

[10]Raouf S.R., "Platinum Supported Zeolite Catalyst Preparation, Characterization and Catalytic Activity ", PhD. Thesis, University of Technology, Baghdad (1994).

[11]Fogler S.C.," Element of Chemical Reaction Engineering", 2nd Edition, Prentice-Hall of India Private Limited, 1997.

[12]Yong H., Hongy S., Jian C.," Modeling, Simulation and Optimization of Commercial Naphtha Catalytic Reforming Process ", Proceeding of the 42nd IEEE Conf, USA, (Dec), p 6206, 2003.

[13]Aguilar R.E., Ancheyta J.J.," New Process Model Proves Accurate in Tests on Catalytic Reformer ", Oil Gas J, vol 25, p 80-83, 1994.

[14]Gates B.C., Katzer J.R., Schuilt G.C.A.," Chemistry of Catalytic Processes", McGraw-Hill book Co. New York, p 184, 1979.

[15]Villafertre E., Jorge A.J.," Kinetic and Reactor Modeling of Naphtha Reforming Process ", J. Petroleum and Coal, vol 44, 1-2, p 63-66, 2002.

[16]Lu H.," Manual of Petrochemical Industry Fundamental Data", Chemical Industry Press, Beijing, China, 1982.

[17]Florence E., Christelle C., Patrice M.," Catalytic Properties in n-heptane Reforming of Pt-Sn and Pt-Ir-Sn/ γ-AL_2O_3 Catalysts Prepared by Surface Redox Reaction", J. Appl. Catalysis A: vol 295, p 157-169, 2005.

[18]Vanina A.M., Javier M.G., Carlos R.V., Juan C.Y., José M.P., Carlos C.Y.," Role of Sn in Pt-Re-Sn/AL_2O_3-Cl Catalysts for Naphtha Reforming ", J. Catal Today, vol 107-108, p 643-650, 2005.

[19]Hyun C.K., Hae S.Y., Lee Turpin A.L., Nam S.P.,"A Reformer Model for a Petrochemicals Complex: PTQ Spring, 2001.

[20]Ali S.A., Siddiqui M.A.," Parametric Study of Catalytic Reforming Process", J. React .Kinet. Catal. Litt, vol 87, (No 1), p 199-206, 2006.

[21]Jorge A.J., Enrique A.R.," New Model Accurately Predicts Reformer Composition", Oil and Gas J, Jan 31, p 93-95, 1994.

[22]Jorge A.J., Eduardo V.M., " Kinetic Modeling of Naphtha Catalytic Reforming Reactions ", J. Energy Fuels, vol 14, No 5, p 1032-1037, 2000.

Nomenclature

Symbol	Definition	Units	Symbol	Definition	Units
A	Aromatics	(-)	$\mathbf{K_{eq}}$	Reaction equilibrium constant	(-)
$\mathbf{A_\circ}$	Pre-exponential factor	(-)	**LHSV**	Liquid hour space velocity	hr^{-1}
$\mathbf{A_i}$	Aromatics(6,7,8,9) carbon atom	(-)	**MW**	Molecular weight	g/gmole
$\mathbf{C_N}$	Naphthenes concentration	$mole/cm^3$	$\mathbf{N_i}$	Naphthene (5,6,7,8,9) carbon atom	(-)
$\mathbf{C_{n\bullet}}$	Initial concentration of species n	$mole/cm^3$	$\mathbf{n\text{-}P_i}$	Paraffine(5,6,7,8,910)carbon atom	(-)
$\mathbf{C_n}$	Concentration of species n	$mole/cm^3$	**P**	Paraffin	(-)
Cp	Specific heat	J/mole.°C	$\mathbf{P_a}$	Total pressure	atm
Ea	Activation energy	kJ/mole	**R**	Gas constant	J/mole.K
$\mathbf{F_{A\bullet}}$	Molar flow rate of component A	mole/hr	$\mathbf{r_i}$	Reaction rate of species i	mole/gcat. hr
$\mathbf{F_{n\bullet}}$	Initial molar flow rate of species n	mole/hr	$\mathbf{r_1}$	Reaction rate for paraffin's dehydrocyclization reaction	mole/gcat. hr
$\mathbf{F_n}$	Molar flow rate of species n	mole/hr	$\mathbf{r_2}$	Reaction rate for naphthene's dehydrogenation reaction	mole/gcat. hr
f	Volumetric flow rate	cm^3 / hr	$\mathbf{r_3}$	Reaction rate for paraffin's hydrocracking reaction	mole/gcat. hr
G	Gases	(-)	**T**	Reaction temperature	°C
GC	Gas chromatography	(-)	$\mathbf{T^\bullet}$	Initial temperature	°C
$\mathbf{H_2}$	Hydrogen	(-)	**V**	Volume of gas adsorbed at the equilibrium pressure	cm^3

ΔH°_r	Heat of i th reaction	J/ mole	$V_{\circ}$	Volume of gas adsorbed by the sample	cm^3
H_2/H.C	Hydrogen to hydrocarbon mole ratio	(-)	V_C	Volume of catalyst	cm^3
iso-P	Iso-paraffins	(-)	W	Weight of catalyst	kg
k	Reaction rate constant	hr^{-1}	WHSV	Weight hour space velocity	hr^{-1}
k_1	Rate constant for paraffin's cyclization	hr^{-1}	Y_i	Molar composition of species i (A, N, and P)	(-)
k_2	Rate constant for naphthenes dehydrogenation	hr^{-1}	zt	Length of reactor	cm
k_3	Rate constant for naphthenes hydroisomerization	hr^{-1}	Δz	Integration step for the reactor length	(-)
k_4	Rate constant for paraffins hydrocracking	hr^{-1}			

Table (1): show the results of analysis of heat of reaction

ΔH°_r (J/mole H_2)				
Reaction	**480 ̊C**	**490 ̊C**	**500 ̊C**	**510 ̊C**
$N + H_2 \rightarrow P$	**-54393.3**	**54238.5**	**-53903.7**	**-53648.5**
$N \rightarrow A + 3H_2$	**73119.9**	**73207.8**	**73291.5**	**73361.2**
$P + (n-3/3)\ H_2 \rightarrow n/15(C_1-C_5)$	**-52623.1**	**-52837.6**	**-53079.3**	**-53309.7**

Table (2): The properties of heavy naphtha (Al-Dura refinery)

Property	Unit	Data
Specific Gravity at 15.6 ˚C	-	0.733
API	-	61.7
Distillation		
I.B.P	°C	60
10 vol % distilled	°C	88
20 vol% distilled	°C	94
30 vol% distilled	°C	106
40 vol% distilled	°C	110
50 vol % distilled	°C	117
60 vol% distilled	°C	124
70 v0l% distilled	°C	132
80 vol% distilled	°C	140
90 vol % distilled	°C	147
F.B.P	°C	178
Total distillate	vol%	98.5
Total recovery	vol%	99.5
Residue	vol%	1

Loss	vol%	0.5
Sulfur Content	ppm	3
Mwt.	g/gmol	108
Total Paraffin	vol %	60
Total naphthene and aromatic Aromatics	vol % vol %	40 < 13

Table (3): Physical and chemical properties of catalyst.

Prepared Pt-Ir-Sn/γ-Al_2O_3	**Prepared Pt-Re-Sn/γ-Al_2O_3**	**Commercial Pt-Re/γ-Al_2O_3**	**Commercial Pt/γ-Al_2O_3**	
0.35	0.3	0.3	0.35	**Pt , wt %**
-	0.3	0.3	-	**Re, wt %**
0.3	0.1	-	-	**Sn ,wt %**
0.1	-	-	-	**Ir , wt %**
Extrudate	Extrudate	Extrudate	Extrudate	**Form**
193.5	196	220	220	**Surface Area m^2 / g**
0.85	0.73	0.6	0..57	**Pore Volume ^{3} / g**
0.691	0.685	0.69	0.66	**Bulk Density g / cm^3**

Table (4): Gas chromatograph analysis condition

Temperature program for the column	
Initial temperature	45 °C
Final temperature	225 °C
Hold time	4 min
Rate of temperature	4 °C/min
Total time	34 min
Other condition	
Pressure at the inlet column	1atm
Pressure of hydrogen	0.3 atm
Injection temperature	225 °C
Pressure of carrier gas N_2	5 atm
Linear velocity	31.3 cm/min
Split ratio	100

Table (5): Retention time of reactants and products in catalytic reforming of heavy naphtha reaction.

Component	Retention time(min)	Component	Retention time(min)
iso-pentane	2.047	iso-octane	5.80
n-pentane	2.123	n-octane	6.58
2,3 diethyl butane	2.280	N_8	7.45
2-methylpentane	2.710	ethyl benzene	7.81
n-hexane	2.543	meta-xylene	8.09
cyclohexane	3.223	para-xylene	8.59
methycyclopentane	3.540	Ortho-xylene	9.50
benzene	3.701	iso-decane	8.93
iso-heptane	4.099	n-decane	10.27
n-heptane	4.480	N_9	11.00
N_7	4.900	A_9	11.31
toluene	5.210	N_{10}	12.64

Table (6) Activation energy values and pre-exponential factor for tri-metal catalysts.

$A_\circ$	Ea kcal/mol	Ea/R	Reaction
Pt-Re-Sn/γ-Al_2O_3			
$2.347*10^{10}$	35.29	17764	**P → N + H_2**
$2.023*10^{7}$	26.56	13367	**N + H_2 → P**
$1.581*10^{5}$	15.863	7983.6	**N → A + 3H_2**
$5.424*10^{7}$	27.19	13684	**P + H_2 → 2G**
Pt-Ir-Sn/γ-Al_2O_3			
$3.626*10^{10}$	36.21	18225	**P → N + H_2**
$3.080*10^{7}$	27.45	13816	**N + H_2 → P**
$7.637*10^{5}$	18.14	9131.5	**N → A + 3H_2**
$2.925*10^{8}$	29.96	15080	**P + H_2 → 2G**

Table (7): **The comparison between theoretical and experimental conversions for tri-metal catalyst at constant WHSV ($1hr^{-1}$) for different reaction temperatures.**

Condition	Components	Pt-Re-Sn/ γ-Al_2O_3		Relative deviation %	Pt-Ir-Sn/ γ-Al_2O_3		Relative deviation %
		Exp. Conv %	Theo. Conv %		Exp. Conv %	Theo. Conv %	
480 °C	**Paraffins**	5.50	6.21	11.43	4.87	5.20	6.35
490 °C	**Paraffins**	6.94	8.09	14.21	6.16	6.85	10.07
500 °C	**Paraffins**	9.44	10.44	9.58	8.62	8.93	3.47
510 °C	**Paraffins**	11.74	13.32	11.86	11.18	11.52	2.95
480 °C	**Naphthenes**	45.60	50.94	10.48	48.44	53.65	9.71
490 °C	**Naphthenes**	45.57	53.85	15.37	48.74	57.55	15.31
500 °C	**Naphthenes**	48.07	56.32	14.65	52.96	61.03	13.22
510 °C	**Naphthenes**	48.10	58.3	17.50	51.52	64.01	19.5
480 °C	**Aromatics**	1.582	1.779	11.10	1.616	1.791	9.77
490 °C	**Aromatics**	1.662	1.863	10.79	1.662	1.880	11.7
500 °C	**Aromatics**	1.80	1.955	7.94	1.839	1.976	6.93
510 °C	**Aromatics**	1.97	2.056	4.18	1.944	2.080	6.54

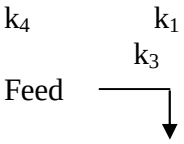

Figure (1) Heavy naphtha reaction network

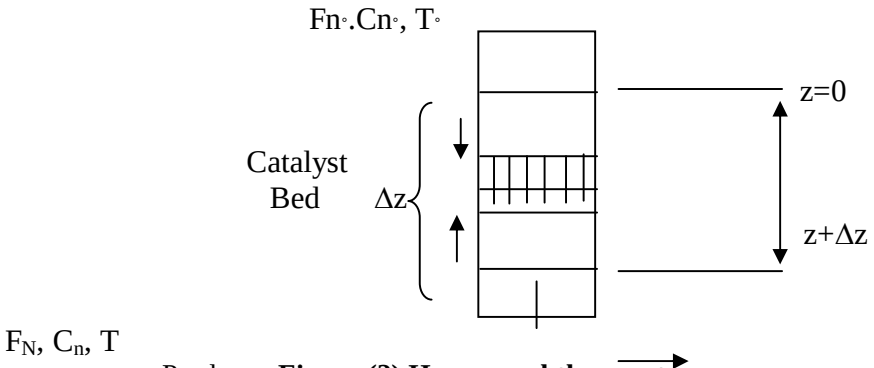

Figure (2) Heavy naphtha reactor

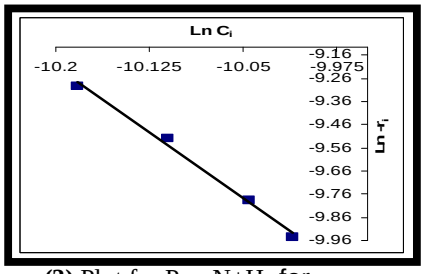

Figure (3) Plot for P↔ N+H_2 for Pt-Ir-Sn catalyst at 1 hr^{-1}

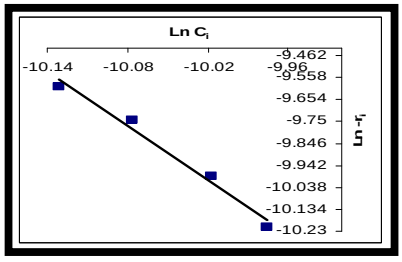

Figure (4) Plot for N→ A+3H_2 for Pt-Re-Sn catalyst at 1.5 hr^{-1}

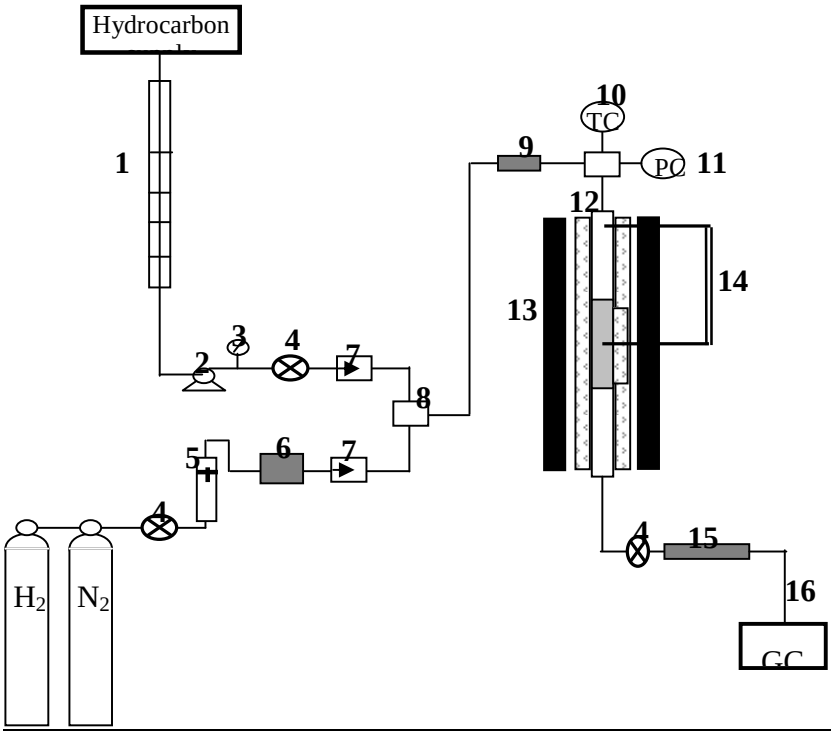

1-Metering burette	**9- Feed preheating zone**
2-Dosing pump	**10 - Temperature controller system**
3-Liquid flow meter	**11- Pressure controller system**
4-Needle valve	**12- Stainless steel reactor**
5- H_2 flow meter	**13- Heating furnace**
6- 5A – Molecular sieve dryer	**14- Thermocouples system**
7- One way value	**15- Cooling system**
8- Mixing section	**16- Gas chromatography**

Figure (5): Schematic diagram of the experimental apparatus catalytic reforming unit

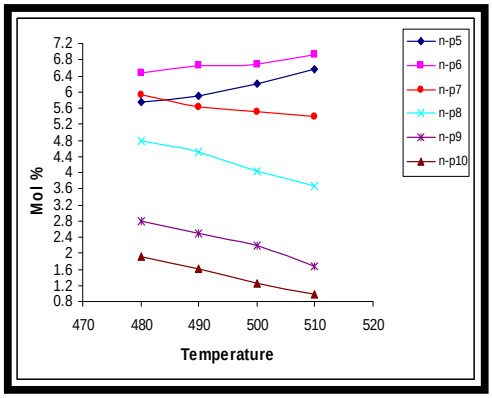

Figure (6) Effect of temperature on the mole % of n-Paraffins components at WHSV of (1 hr^{-1}) for (Pt-Re-Sn / γ-Al_2O_3) catalyst.

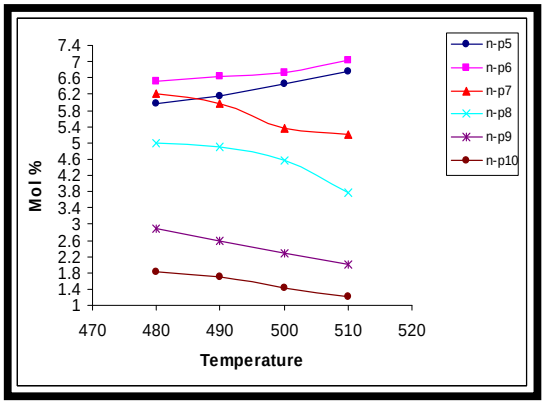

Figure (7) Effect of temperature on the mole % of iso-Paraffins components at WHSV of (1 hr^{-1}) for (Pt-Ir-Sn / γ-Al_2O_3) catalyst.

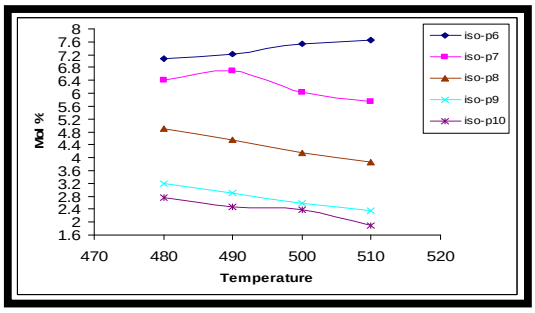

Figure (8) Effect of temperature on the mole % of naphthenes components at WHSV of (1 hr^{-1}) for (Pt-Re-Sn / γ-Al_2O_3) catalyst.

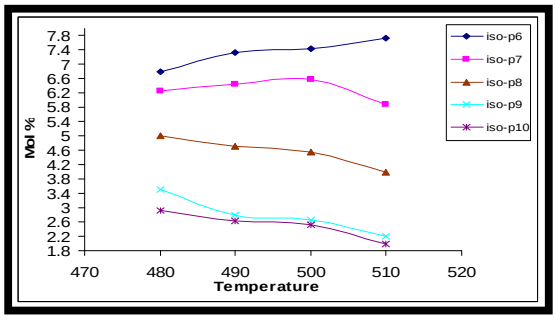

Figure (9) Effect of temperature on the mole % of aromatics components at WHSV of (1 hr^{-1}) for (Pt-Ir-Sn / γ-Al_2O_3) catalyst.

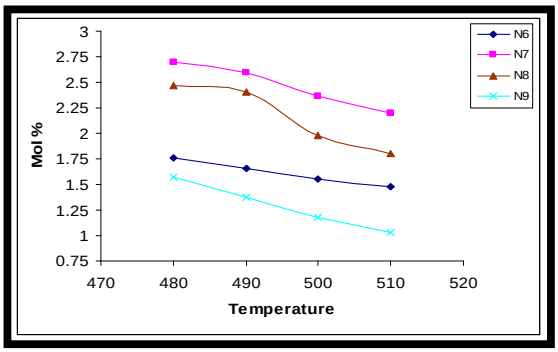

Figure (10) Effect of temperature on the mole % of n-Paraffins components at WHSV of (1 hr^{-1}) for (Pt-Re-Sn / γ-Al_2O_3) catalyst.

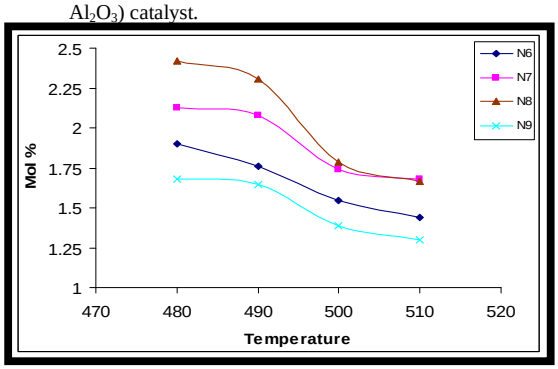

Figure (11) Effect of temperature on the mole % of iso- components at WHSV of (1 hr^{-1}) for (Pt-Ir-Sn / γ- Al_2O_3) catalyst.

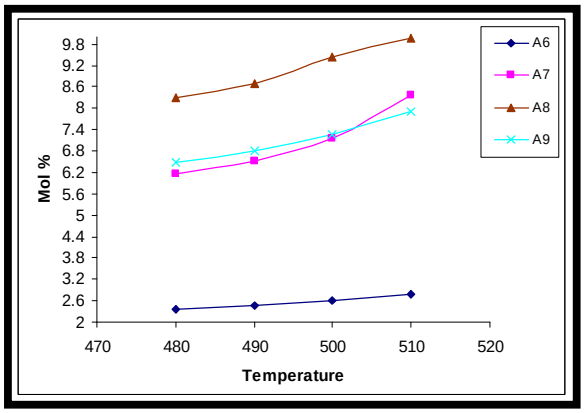

Figure (12) Effect of temperature on the mole % of naphthenes WHSV of (1 hr^{-1}) for (Pt-Re-Sn / γ-Al_2O_3) catalyst.

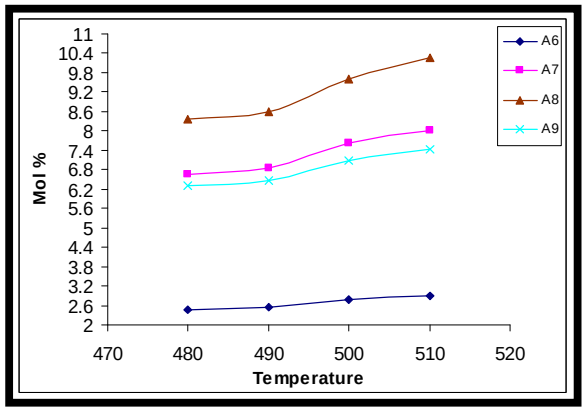

Figure (13) Effect of temperature on the mole % of components at aromatics components at WHSV of (1 hr^{-1}) for (Pt-Ir-Sn / γ- Al_2O_3) catalyst.

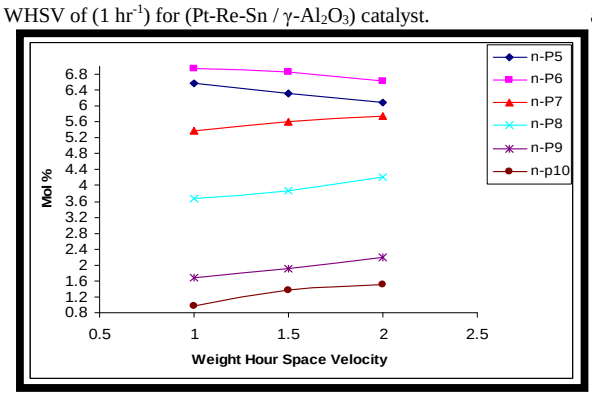

Figure (14) Effect of weight hour space velocity on the mole % of n-Paraffins components at 510 °C for (Pt-Re-Sn / γ-Al_2O_3) catalyst.

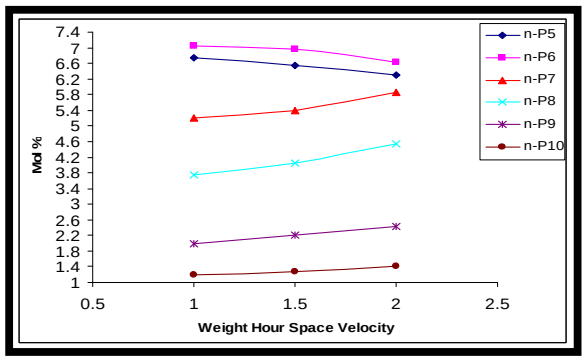

Figure (15) Effect of weight hour space velocity on the mole % of n-Paraffins components at 510 °C for (Pt-Ir-Sn / γ-Al_2O_3) catalyst.

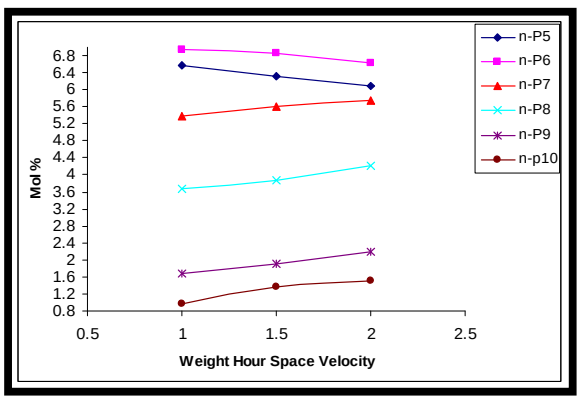

Figure (16) Effect of weight hour space velocity on the mole % of iso-Paraffins components at 510 °C for (Pt-Re-Sn / γ-Al_2O_3) catalyst.

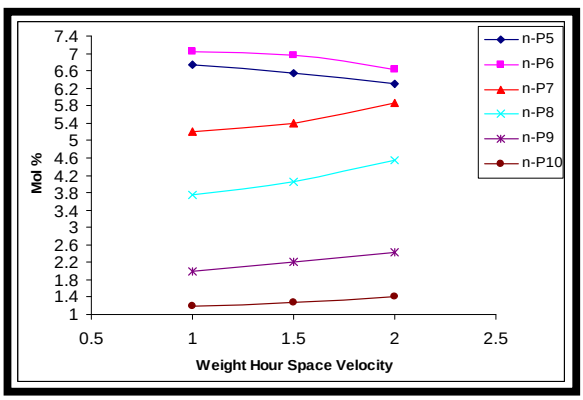

Figure (17) Effect of weight hour space velocity on the mole % of iso-Paraffins components at 510 °C for (Pt-Ir-Sn / γ-Al_2O_3)catalyst.

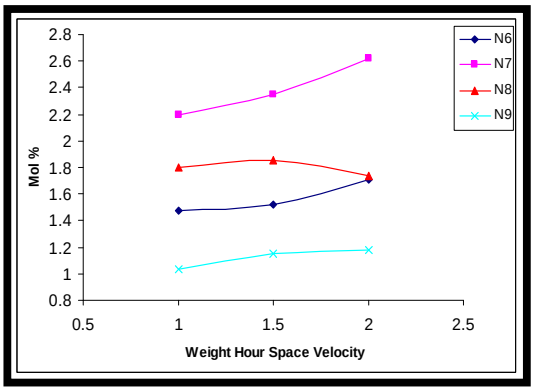

Figure (18) Effect of weight hour space velocity on the mole % naphthenes components at 510 °C for (Pt-Re-Sn / γ-Al_2O_3) of catalyst.

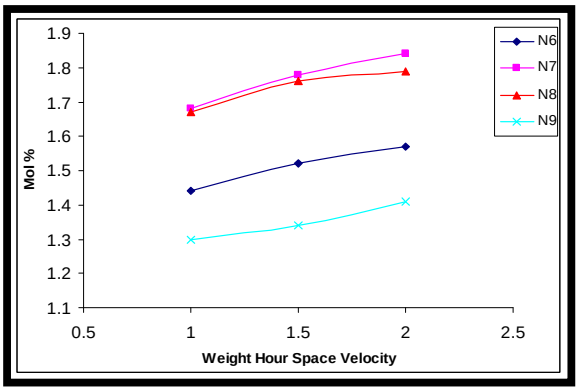

Figure (19) Effect of weight hour space velocity on the mole % naphthenes components at 510 °C for (Pt-Ir-Sn / γ-Al_2O_3) of catalyst.

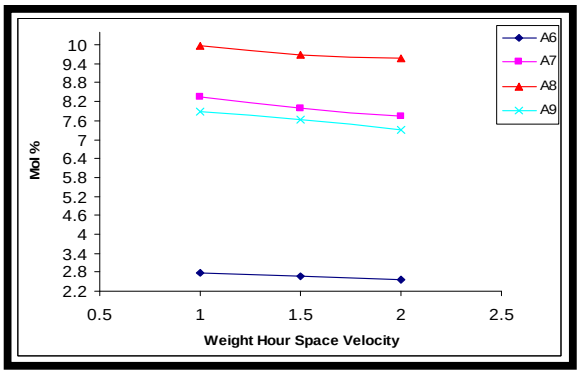

Figure (20) Effect of weight hour space velocity on the mole % aromatics components at 510 °C for (Pt-Re-Sn / γ-Al_2O_3) of catalyst.

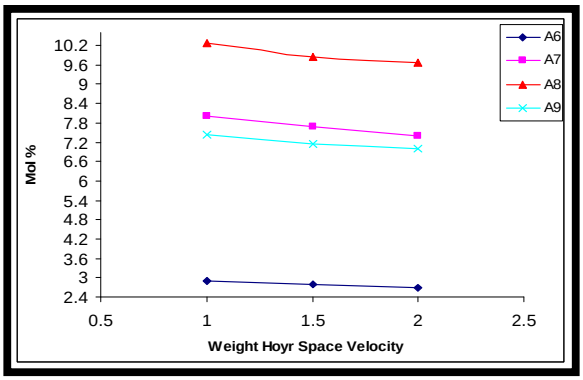

Figure (21) Effect of weight hour space velocity on the mole % aromatics components at 510 °C for (Pt-Ir-Sn / γ-Al_2O_3) of catalyst.

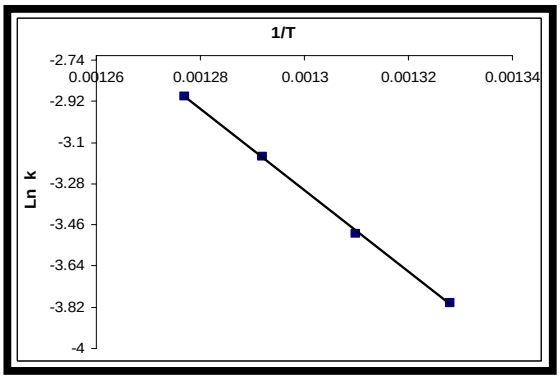

Figure (22) Arrhenius plot for the reaction P → N + H_2 for Pt-Re-Sn/γ-Al_2O_3.

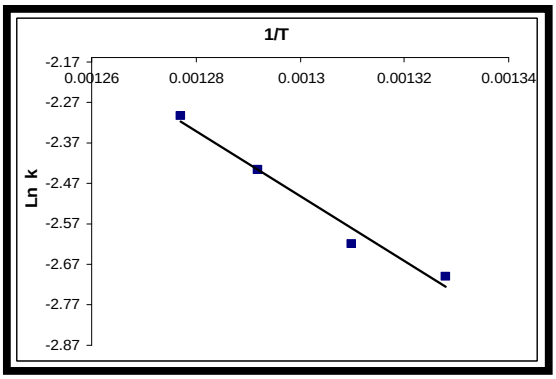

Figure (23) Arrhenius plot for the reaction N→A+3H_2 for Pt-Re-Sn/γ-Al_2O_3.

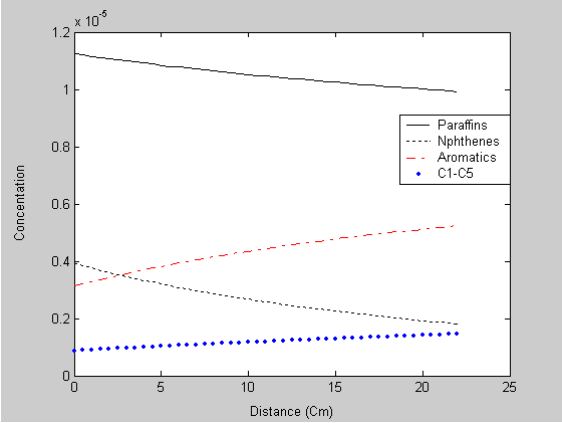

Figure (24) Concentration profiles for (Paraffins, Naphthenes, Aromatics, and gases) at 480 °C and (1 hr^{-1}) for (Pt-Re-Sn / γ-Al_2O_3) catalyst.

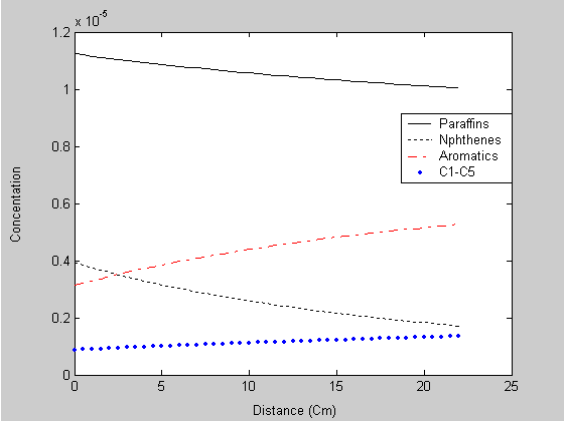

Figure (25) Concentration profiles for (Paraffins, Naphthenes, Aromatics, and gases) at 480 °C and (1 hr^{-1}) for (Pt-Ir-Sn / γ-Al_2O_3) catalyst.

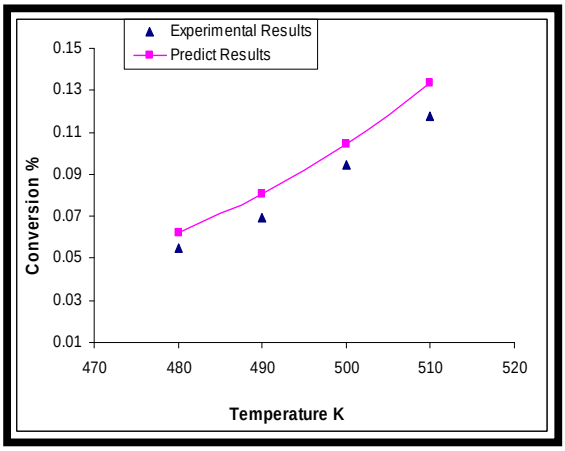

Figure (26) comparison between the experimental and predicted paraffins conversion at WHSV of (1hr^{-1}) for (Pt-Re-Sn / γ-Al_2O_3) catalyst.

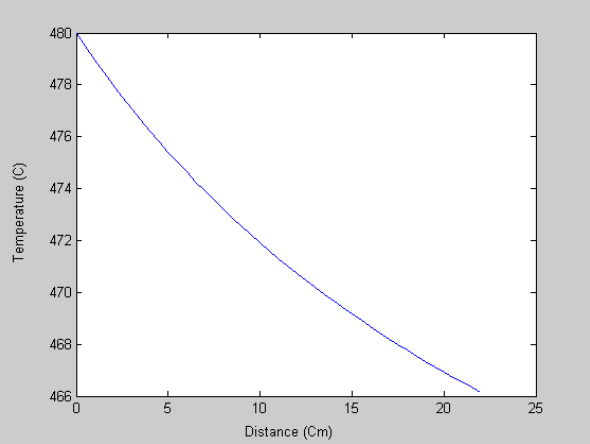

Figure (27) Simulation of temperature profile for (Pt-Re-Sn / γ-Al_2O_3) catalyst at 480 °C and (1hr^{-1}).

.